arXiv:1606.01963v1 [physics.atom-ph] 6 Jun 2016

MDPI

Article

Analysis of polarizability measurements made with atom interferometry

Maxwell D. Gregoire [1], Nathan Brooks [1], Raisa Trubko[2], and Alexander D. Cronin [1,2]*

[1] Department of Physics, University of Arizona, Tucson, Arizona
[2] College of Optical Sciences, University of Arizona, Tucson, Arizona
* Correspondence: cronin@physics.arizona.edu; Tel.: 520-465-8459

Academic Editor: name
Version June 8, 2016 submitted to Atoms; Typeset by LaTeX using class file mdpi.cls

Abstract: We present revised measurements of the static electric dipole polarizabilities of K, Rb, and Cs based on atom interferometer experiments presented in [*Phys. Rev. A* **2015**, 92, 052513] but now re-analyzed with new calibrations for the magnitude and geometry of the applied electric field gradient. The resulting polarizability values did not change, but the uncertainties were significantly reduced. Then we interpret several measurements of alkali metal atomic polarizabilities in terms of atomic oscillator strengths f_{ik}, Einstein coefficients A_{ik}, state lifetimes τ_k, transition dipole matrix elements D_{ik}, line strengths S_{ik}, and van der Waals C_6 coefficients. Finally, we combine atom interferometer measurements of polarizabilities with independent measurements of lifetimes and C_6 values in order to quantify the residual contribution to polarizability due to all atomic transitions other than the principal ns-np_J transitions for alkali metal atoms.

Keywords: atom interferometry; polarizability; oscillator strengths; state lifetimes; dipole matrix elements; line strength; van der Waals interactions

1. Introduction

Atomic and molecular interferometry [1,2] has become a precise method for measuring atomic properties such as static polarizabilities [3–7], van der Waals interactions [8–10], and tune-out wavelengths [11,12]. Calculating these atomic and molecular properties *ab initio* is challenging because it requires modeling of quantum many-body systems with relativistic corrections. For example, different methods for calculating polarizabilities yield results that vary by as much as 10% for Cs [13–41]. For molecules the challenges are even greater. Furthermore, determining the uncertainty for an *ab initio* calculation can be difficult. Polarizability measurements made with matter wave interferometry, therefore, have been used to assess which calculation methods are most valid. Testing these calculations is important because similar methods are used to predict atomic scattering cross sections, Feshbach resonances, photoassociation rates, atom-surface van-der Waals C_3 coefficients, atomic parity-violating amplitudes, and atomic clock shifts due to thermal radiation or collisions.

In this manuscript, we first present revised uncertainties on our most recent K, Rb, and Cs static polarizability measurements [3] in Section 2. We then show how to use polarizability measurements for alkali metal atoms [3–5,7] as input for semi-empirical calculations of atomic properties such as oscillator strengths, Einstein A coefficients, state lifetimes, transition matrix elements, and line strengths, as we discuss in Section 3.1. We use polarizability measurements to predict van der Waals C_6 coefficients in Section 3.2. To support this analysis, throughout Section 3 we use theoretical values for so-called *residual polarizabilities* of alkali metal atoms, i.e. the contributions to polarizabilities that come higher-energy excitations associated with the inner-shell (core) electrons

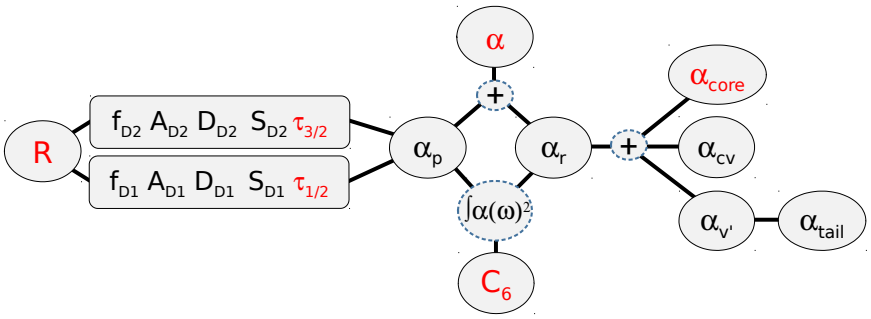

Figure 1. An idea chart showing connections between various quantities defined in Equations (1)-(17) that we relate to static polarizability $\alpha(0)$ for alkali metal atoms. Quantities in red have been directly measured.

and highly-excited states of the valence electrons. The idea-chart in Fig. 1 shows connections between the residual polarizability (α_r) and several quantities related via Eqns. (1)-(17) that we use to interpret polarizabilities.

Then in Section 4 we demonstrate an all-experimental method for measuring residual polarizabilities. We do this by using polarizability measurements in combination with independent measurements of lifetimes and van der Waals C_6 coefficients. This serves as a cross-check for some assumptions used in Section 3 that are also used for analysis of atomic parity violation and atomic clocks. Section 4 highlights how atom interferometry measurements shown in Table 1 are sufficiently precise to directly measure the static residual polarizability, $\alpha_r(0)$, for each of the alkali-metal atoms, Li, Na, K, Rb, and Cs.

2. Revised uncertainties on recent polarizability measurements

We reduced the uncertainties in our most recent K, Rb, and Cs static polarizability measurements [3] to 0.11% by reducing the total systematic uncertainty from 0.15% to 0.10%. In our experiment, we used cylindrical electrodes, indicated in red in Fig. 2, to induce phase shifts in our atom interferometer that are proportional to $\alpha(0)V^2$, the atoms' static polarizabilities times the square of the voltage difference between the electrodes. Fig. 3a shows an example of how the induced phase shift changes as we move the electrodes laterally with respect to the beamline.

We reduced the systematic uncertainty in our measurements from 0.15% to 0.12% by calibrating the voltage supplies connected to the electrodes to 36 ppm using a Vitrek 4700 high-accuracy voltmeter. Each electrode is held at its respective positive or negative voltage with respect to ground by its own power supply. We concluded that when we instructed the power supplies to output ± 6 kV, both power supplies were actually supplying $\pm 6.0026(2)$ kV. Our results agreed with less-accurate calibration measurements of $\pm 6.003(3)$ we made earlier using a Fluke 287 multimeter and a Fluke 80k-40 high-voltage probe. At normal operating temperatures, our calibration measurements were completely reproducible to within the resolution of the Vitrek 4700.

The strength of the electric field gradient, and therefore the magnitude of the induced phase shift, also depends on the distance between the electrodes. In the past, we measured that distance to be 1999.9(5) μm by sweeping the electrodes across the beamline and measuring the lateral positions at which the electrodes eclipsed the beam (see an example of these data in Fig. 3b). We found that scatter in our measurements was explained by misalignment of the collimating slits and detector. After correcting for this source of error, we measured the distance between electrodes to be 1999.7(2) μm, which further reduced our total systematic uncertainty from 0.12% to 0.10%. Our measurements did not change as a function of maximum atom flux, electrodes translation motor speed, atom beam y position or vertical collimation, atom beam velocity, or atomic species.

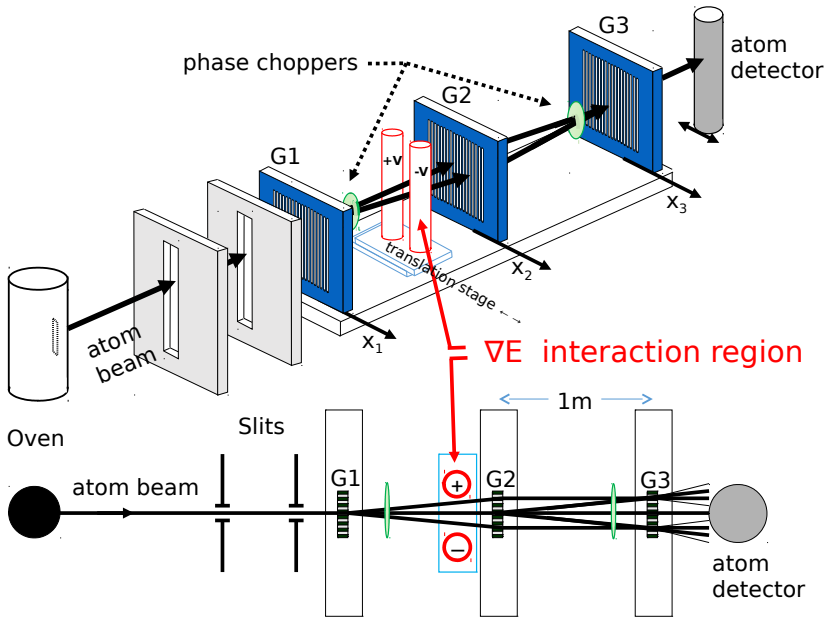

Figure 2. Diagram of the atom interferometer we used to measure the static polarizabilities of K, Rb, and Cs [3]. A pair of cylindrical, oppositely-charged electrodes, indicated in red, induce phase shifts that depend on atoms' polarizabilities and the gradient of the produced electric field.

By themselves, the new values we measured for the electrodes' voltages and the distance between the electrodes changed our reported polarizabilities by +140 ppm and -140 ppm, respectively. Therefore, the polarizability values that we report are the same as those in [3] but with smaller uncertainties. It is also worth noting that either of the $\pm$140 ppm changes, by itself, would still not have been statistically significant. These reduced total uncertainties are shown alongside the previously-reported values in Table 1.

3. Analysis of atom interferometry polarizability measurements

Table 1 lists polarizability measurements made with atom interferometry. For Li, Na, K, Rb, and Cs, atom interferometry has provided the best available measurements. Polarizability measurements made using other methods are reviewed in [13,42–46].

The original references [3,4,7] show how the polarizability measurements in Table 1 compare to theoretical predictions [13,19–41]. In this article, we devote our attention to interpreting the atomic polarizability measurements in Table 1 in a systematic and tutorial manner. In the rest of Section 3 we show how to use these polarizability measurements to predit other atomic properties such as oscillator strengths, lifetimes, matrix elements, line strengths, and van der Waals C_6 coefficients, following procedures described earlier by Derevianko and Porsev [47], Amini and Gould [42], and Mitroy, Safronova, and Clark [13] among others. Then, in Section 4, we use the polarizabilities in Table 1 to provide experimental constraints on the residual polarizabilities, α_r, for each of the alklai atoms.

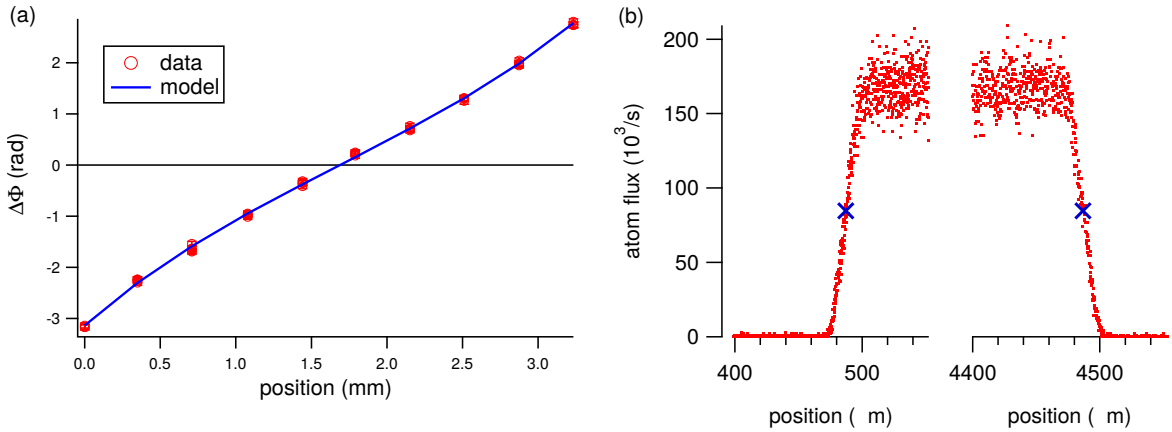

Figure 3. (a): Induced phase shift in the interferometer vs the lateral position of the electrodes with respect to the beam. (b): Observed atom beam flux as a function of the electrodes' lateral position. We use these data to determine the distance between the electrodes.

Table 1. Measurements of static polarizabilities $\alpha(0)$ made using atom or molecule interferometry. References [4,5] used a septum electrode and references [3,6,7] used electric field gradients to shift the phase of matter wave interference fringes. Results are presented both in Å^3 and atomic units (au). Values we use for analysis in this paper are in bold.

Atom or molecule	**Polarizability** (Å^3)	(au)	**Reference**	**Uncertainty**
Li	**24.33(16)**	**164.2(11)**	[5]	0.66%
Na	**24.11(8)**	**162.7(5)**	[4]	0.35%
Na	24.11(18)	162.7(12)	[7]	0.75%
K	43.06(21)	290.6(14)	[7]	0.49%
K	42.93(7)	289.7(5)	[3]	0.16%
K	**42.93(5)**	**289.7(3)**	this work	0.11%
Rb	47.24(21)	318.8(14)	[7]	0.44%
Rb	47.39(8)	319.8(5)	[3]	0.17%
Rb	**47.39(5)**	**319.8(3)**	this work	0.11%
Cs	59.39(9)	400.8(6)	[3]	0.15%
Cs	**59.39(6)**	**400.8(4)**	this work	0.11%
C_{60}	88.9(52)	600(35)	[6]	5.9%
C_{70}	108.5(65)	732(44)	[6]	6.5%

3.1. Reporting oscillator strengths, lifetimes, matrix elements, and line strengths from static polarizabilities

The dynamic polarizability, $\alpha(\omega)$, of an atom in state $|i\rangle$ can be written as a sum over electric-dipole transition matrix elements $\langle k|e\vec{r}|i\rangle$, Einstein coefficients A_{ik}, oscillator strengths f_{ik}, or line strengths S_{ik} as

$$\alpha(\omega) = \frac{e^2}{m}\sum_{k\neq i}\frac{f_{ik}}{\omega_{ik}^2-\omega^2} \tag{1}$$

$$\alpha(\omega) = 2\pi\epsilon_0 c^3\sum_{k\neq i}\frac{A_{ki}\omega_{ik}^{-2}}{\omega_{ik}^2-\omega^2}\frac{g_k}{g_i} \tag{2}$$

$$\alpha(\omega) = \frac{2}{3\hbar}\sum_{k\neq i}\frac{|\langle k|e\vec{r}|i\rangle|^2\omega_{ik}}{\omega_{ik}^2-\omega^2} \tag{3}$$

$$\alpha(\omega) = \frac{1}{3\hbar}\sum_{k\neq i}\frac{S_{ik}\omega_{ik}}{\omega_{ik}^2-\omega^2} \tag{4}$$

where e and m are the charge and mass of an electron, $\omega_{ik} = (E_k - E_i)/\hbar$ are resonant frequencies for excitation from state $|i\rangle$ to state $|k\rangle$, and $g_k = 2J_k + 1$ is the degeneracy of state $|k\rangle$. The squares of electric dipole transition matrix elements $|\langle k|e\vec{r}|i\rangle|^2$, or equivalently $3|\langle k|e\vec{x}|i\rangle|^2$, are related to the reduced dipole matrix elements (denoted with double bars) by $|\langle k\|e\vec{r}\|i\rangle|^2 = |D_{ik}|^2 = \sum_{m_k,m_i}|\langle k|e\vec{r}|i\rangle|^2 = |\langle k|e\vec{r}|i\rangle|^2 g_i$ using the Wigner-Eckart theorem. For ground state alkali atoms, line strength $S_{ik} = |D_{ik}|^2$.

The expressions for polarizability $\alpha(0)$ in Eqs. (1) - (4) each have dimensions of $4\pi\epsilon_0$ times volume, as expected from the definitions $\vec{p} = \alpha\vec{E}$ and $U = -\frac{1}{2}\alpha|\vec{E}|^2$, where $\vec{p}$ is the induced dipole moment and U is the energy shift (Stark shift) of an atom in an electric field $\vec{E}$. When polarizability is reported in units of volume (typically Å^3 or 10^{-24} cm^3) it is implied that one can multiply by $4\pi\epsilon_0$ to get polarizability in SI units. The atomic unit (au) of polarizability, $e^2a_0^2/E_h$, is equivalent to $a_0^3\times 4\pi\epsilon_0$, where a_0 is the Bohr radius, and E_h is a Hartree. Since $(4\pi\epsilon_0) = 1$ in au, polarizability is naturally expressed in atomic units of volume of a_0^3 (and for reference $a_0^3 = 0.148185$ Å^3).

Since the principal D1 and D2 transitions of alkali metal atoms (denoting the ns-$np_{1/2}$ and ns-$np_{3/2}$ transitions respectively, where n=6 for Cs, n=5 for Rb, n=4 for K, n=3 for Na, and n=2 for Li), account for over 95% of those atoms' static polarizabilities [33], it is customary to decompose polarizability as

$$\alpha(\omega) = \alpha_p(\omega) + \alpha_r(\omega) \tag{5}$$

where $\alpha_p(\omega)$ represents the contribution from the principal transitions and $\alpha_r(\omega)$ is the residual polarizability due to all other excitations. The residual polarizability itself can be further decomposed as

$$\alpha_r(\omega) = \alpha_{v'}(\omega) + \alpha_{\rm core}(\omega) + \alpha_{cv}(\omega) \tag{6}$$

where $\alpha_{v'}$ is due to higher $ns_{1/2} - n'p_J$ excitations of the valence electron with $n' > n$, $\alpha_{\rm core}$ is the polariability due to the core electrons, and α_{cv} is due to correlations between core and valence electrons. Sometimes the notation $\alpha_{\rm tail}$ is used to denote a subset of $\alpha_{v'}$ with $n' > (n+3)$ [48], or $n' > (n+5)$ [32], or an even higher cutoff such as $n' > 26$ [40].

Using the decomposition in Eqn. (5) we can rewrite Eqs. (1)-(4) for static ($\omega = 0$) polarizabilities:

$$\alpha(0) = \frac{e^2}{m}\left[\frac{f_{D1}}{\omega_{D1}^2} + \frac{f_{D2}}{\omega_{D2}^2}\right] + \alpha_r(0) \tag{7}$$

$$\alpha(0) = 2\pi\epsilon_0 c^3\left[\frac{\tau_{1/2}^{-1}}{\omega_{D1}^4} + 2\frac{\tau_{3/2}^{-1}}{\omega_{D2}^4}\right] + \alpha_r(0) \tag{8}$$

$$\alpha(0) = \frac{1}{3\hbar}\left[\frac{|D_{D1}|^2}{\omega_{D1}} + \frac{|D_{D2}|^2}{\omega_{D2}}\right] + \alpha_r(0) \tag{9}$$

$$\alpha(0) = \frac{1}{3\hbar}\left[\frac{S_{D1}}{\omega_{D1}} + \frac{S_{D2}}{\omega_{D2}}\right] + \alpha_r(0) \tag{10}$$

Eqn. (8) is written in terms of lifetimes $\tau_k^{-1} = \sum_i A_{ki}$, rather than Einstein A coefficients because alkali metal atom np_J states decay with a branching ratio of 100% to their respective ground $ns_{1/2}$ states. To support our analysis of polarizabilites here in Section 3 we use theoretically caclulated values of residual static polarizabilities $\alpha_r(0)$ = 2.04(69) au for Li, $\alpha_r(0)$ = 1.86(12) au for Na, $\alpha_r(0)$ = 6.26(33) au for K, $\alpha_r(0)$ = 10.54(60) au for Rb, all from Savronova et *al.* [48], and $\alpha_r(0)$ = 16.74(11) au for Cs from Derevianko et *al.* [47]. Table 6 in Appendix A lists these and several other published values for $\alpha_{\rm core}(0)$, $\alpha_{v'}(0)$, $\alpha_{cv}(0)$ and $\alpha_r(0)$.

Since ω_{D1} and ω_{D2} are well known [49], we can further use Eqs. (7)-(10) to derive expressions for $|D_{ik}|^2$, τ_k, and f_{ik} in terms of $\alpha(0)$, $\alpha_r(0)$, and a ratio of line strengths R:

$$f_{D1} = \frac{[\alpha(0) - \alpha_r(0)]}{\left(\frac{e^2}{m\omega_{D1}^2}\right)}\left(\frac{1}{1 + R\frac{\omega_{D1}}{\omega_{D2}}}\right) \tag{11}$$

$$f_{D2} = \frac{[\alpha(0) - \alpha_r(0)]}{\left(\frac{e^2}{m\omega_{D1}^2}\right)}\left(\frac{R}{\frac{\omega_{D2}}{\omega_{D1}} + R}\right) \tag{12}$$

$$\tau_{1/2} = \frac{2\pi\epsilon_0 c^3\omega_{D1}^{-3}}{[\alpha(0) - \alpha_r(0)]}\left(\frac{1}{\omega_{D1}} + \frac{R}{\omega_{D2}}\right) \tag{13}$$

$$\tau_{3/2} = \frac{2\pi\epsilon_0 c^3\omega_{D2}^{-3}}{[\alpha(0) - \alpha_r(0)]}\left(\frac{2}{R\omega_{D1}} + \frac{2}{\omega_{D2}}\right) \tag{14}$$

$$|D_{D1}|^2 = S_{D1} = [\alpha(0) - \alpha_r(0)]\left(\frac{3\hbar}{\frac{1}{\omega_{D1}} + \frac{R}{\omega_{D2}}}\right) \tag{15}$$

$$|D_{D2}|^2 = S_{D2} = [\alpha(0) - \alpha_r(0)]\left(\frac{3\hbar}{\frac{1}{R\omega_{D1}} + \frac{1}{\omega_{D2}}}\right) \tag{16}$$

where R is defined as

$$R \equiv \frac{S_{D2}}{S_{D1}} = \frac{|D_{D2}|^2}{|D_{D1}|^2} = \frac{f_{D2}}{f_{D1}}\frac{\omega_{D1}}{\omega_{D2}} = 2\frac{\tau_{1/2}}{\tau_{3/2}}\left(\frac{\omega_{D1}}{\omega_{D2}}\right)^3 \tag{17}$$

To support our analysis of polarizabilities, we will use R= 2.0000 for Li inferred from [18], R=1.9994(37) for Na [50], R=1.9976(13) for K [51], R=1.99219(3) for Rb [12] , and R= 1.9809(9) for Cs [52]. It is noteworthy that references [11,12,51] determined R experimentally using atom interferometry measurements of tune-out wavelengths.

Table 2 shows principal transition matrix elements, lifetimes, line strengths, and oscillator strengths inferred from polarizability measurements using Eqns. (11)-(17). Our inferred lifetimes for K, Rb, and Cs are based on $\alpha(0)$ measurements with 0.11% uncertainty, yet our derived lifetimes have slightly larger uncertainty. In the case of Li, Na, K and Rb, this is because roughly half of the total

Table 2. Atomic properties inferred from atom interferometry measurements [3–5]. Reduced matrix elements $D_{D1} = \langle np_{1/2}\|r\|ns_{1/2}\rangle$ and $D_{D2} = \langle np_{3/2}\|r\|ns_{1/2}\rangle$, lifetimes $\tau_{np1/2}$ and $\tau_{np3/2}$, oscillator strengths f, and line strengths S shown here are inferred from measurements of polarizabilities, $\alpha(0)$ shown in Table 1 using Eqns (11) - (16). Subscripts D1 and D2 refer to the ns-$np_{1/2}$ and ns-$np_{3/2}$ transitions respectively, where n=6 for Cs, n=5 for Rb, n=4 for K, n=3 for Na and n=2 for Li. Uncertainty budget components δ_α, δ_R, and δ_{α_r} come from the uncertainties in $\alpha(0)$ [3–5] (see Table 1), R [12,18,50–52], and $\alpha_r(0)$ [47,48] (see Table 6). The resulting uncertainties for D_{D1}, D_{D2}, $\tau_{np1/2}$, $\tau_{np3/2}$, f_{D1}, f_{D2}, S_{D1}, and S_{D2} are reported presuming possible errors δ_α, δ_R, and δ_{α_r} are uncorrelated. The symbol (-) indicates an uncertainty < 1 in the least significant digit.

atom	D_{D1} (au)	δ_α	δ_R	δ_{α_r}	D_{D2} (au)	δ_α	δ_R	δ_{α_r}
Li	3.318(13)	(11)	(-)	(7)	4.693(19)	(16)	(-)	(10)
Na	3.527(6)	(6)	(2)	(1)	4.987(8)	(8)	(2)	(2)
K	4.101(4)	(3)	(1)	(2)	5.800(5)	(4)	(1)	(3)
Rb	4.239(5)	(3)	(-)	(4)	5.989(7)	(4)	(-)	(6)
Cs	4.508(3)	(3)	(1)	(1)	6.345(4)	(4)	(-)	(1)
atom	$\tau_{1/2}$ (ns)	δ_α	δ_R	δ_{α_r}	$\tau_{3/2}$ (ns)	δ_α	δ_R	δ_{α_r}
Li	27.08(21)	(18)	(-)	(11)	27.08(21)	(18)	(-)	(11)
Na	16.28(6)	(5)	(2)	(3)	16.24(5)	(5)	(1)	(1)
K	26.80(4)	(3)	(1)	(3)	26.45(4)	(3)	(1)	(3)
Rb	27.60(6)	(3)	(-)	(5)	26.14(6)	(3)	(-)	(5)
Cs	34.77(5)	(5)	(1)	(1)	30.37(5)	(4)	(1)	(-)
atom	f_{D1}	δ_α	δ_R	δ_{α_r}	f_{D2}	δ_α	δ_R	δ_{α_r}
Li	0.2492(20)	(17)	(-)	(11)	0.4985(39)	(33)	(-)	(39)
Na	0.3203(12)	(11)	(4)	(2)	0.6410(23)	(22)	(4)	(5)
K	0.3317(6)	(4)	(1)	(4)	0.6665(11)	(8)	(1)	(7)
Rb	0.3438(8)	(4)	(-)	(7)	0.6982(17)	(9)	(-)	(14)
Cs	0.3450(5)	(5)	(1)	(1)	0.7174(10)	(10)	(1)	(2)
atom	S_{D1} (au)	δ_α	δ_R	δ_{α_r}	S_{D2} (au)	δ_α	δ_R	δ_{α_r}
Li	11.01(9)	(8)	(-)	(5)	22.02(17)	(15)	(-)	(9)
Na	12.44(5)	(4)	(2)	(1)	24.87(8)	(8)	(2)	(2)
K	16.82(3)	(2)	(1)	(2)	33.64(6)	(4)	(1)	(4)
Rb	17.97(4)	(3)	(-)	(3)	35.87(8)	(4)	(-)	(7)
Cs	20.32(3)	(3)	(1)	(1)	40.26(5)	(5)	(1)	(1)

Table 3. Cesium $6p_J$ lifetimes (τ_J) from several references, tabulated here for comparison. The $\tau_{2/1}$ and $\tau_{3/2}$ values that we report using $\alpha(0)$ measured by atom interferometry et *al.* [3] (combined with values of $\alpha_r(0)$ [61] and R [52]) are reproduced from Table 2. Similar comparisons appear in Table II of [42] and Table I of [63].

$\tau_{1/2}$ (ns)	$\tau_{3/2}$ (ns)	Method and Reference(s)
34.77(5)	30.37(5)	this work using $\alpha(0)$ from atom interferometry [3]
34.75(5)	30.35(5)	this approach using $\alpha(0)$ from [42]
34.76(3)	30.36(3)	this approach using $\alpha(0)$ from both [3] and [42]
35.07(10)	30.57(7)	[59] Rafac 1999
34.93(10)	30.50(7)	[57] Rafac 1994
34.75(7)	30.41(10)	[58] Young 1994
34.80(7)	30.39(6)	[60] Derevianko 2002
34.883(53)	30.462(46)	$\tau_{3/2}$ from [63], combined with R [52] to infer $\tau_{1/2}$
34.755	30.3502	from D_{D1} calculation by [61], combined with R [52] to infer $\tau_{3/2}$

uncertainty comes from uncertainty in $\alpha_r(0)$, whereas for Cs the uncertainties in τ are dominated by contributions from uncertainty in $\alpha(0)$. Because there have been many high precision measurements of alkali metal principal transition lifetimes, it is useful to compare our derived lifetimes to those measurements. Our derived K and Rb lifetimes agree well with and have comparable uncertainty to those measured by Volz et *al.* [50], Wang et *al.* [53,54], and Simsarian et *al.* [55]. Because the $\alpha(0)$ measurements used to derive the Li and Na lifetimes in Table 2 are less precise, our inferred Na lifetimes have about twice the uncertainty (about 0.4%) of measurements by Volz et *al.* [50], and our inferred Li lifetimes have much greater uncertainty than measurements by Volz et *al.* [50] and McAlexander et *al.* [56].

For Cs, the lifetimes we report in Table 2 for this work have an uncertainty of less than 0.15%, which is slightly smaller than the uncertainty of four previous high-precision determinations of the Cs $6p_J$ state lifetimes [57–60]. Table 3 and Fig. 4 show how our lifetime results are consistent with [58,60] but differ from lifetimes reported in [57,59]. Our results deviate by 1.5σ from $\tau_{1/2}$ found in [57] and by 3σ from $\tau_{1/2}$ in [59], where σ for the deviations here refers to the combined uncertainty (added in quadrature) for the experiments. Comparing the sum of line strengths ($S_{D1} + S_{D2}$), a quantity that is mostly independent of R, provides a similar conclusion: our results are consistent with [58] and [60] but differ by two and three σ from [57] and [59].

Because the two recent measurements of $\alpha_{\mathrm{Cs}}(0)$ by Gregoire et *al.* [3] and Amini and Gould [42] were made using very different methods, we combine these measurements using a weighted average in order to report a value for $\tau_{6p_{1/2},\mathrm{Cs}}$ with even smaller (0.03 ns) uncertainty in Table 3. We note that, due to the uncertainty in R and $\alpha_r(0)$, the uncertainty in $\tau_{6p_{1/2},\mathrm{Cs}}$ would still be 0.01 ns even if the polarizability measurements had no uncertainty.

The Cs $|D_{D1}|$ value calculated *ab initio* by [61] is also consistent with our results for $|D_{D1}|$. Since our results come from independent measurements of $\alpha(0)$ and R, combined with theoretical values for $\alpha_r(0)$, the agreement between our result for $|D_{D1}|$ with the that of Derevianko and Porsev [60,61] adds confidence to their analysis of atomic parity violation [61,62].

3.2. Deriving van der Waals coefficients from polarizabilities

Since polarizability determines the strengths of van der Waals (vdW) potentials, we can also use measurements of $\alpha(0)$ to improve predictions for atom-atom interactions. Two ground-state atoms have a van der Waals interaction potential

$$U = -\frac{C_6}{r^6} - \frac{C_8}{r^8} - \frac{C_{10}}{r^{10}} + ... \tag{18}$$

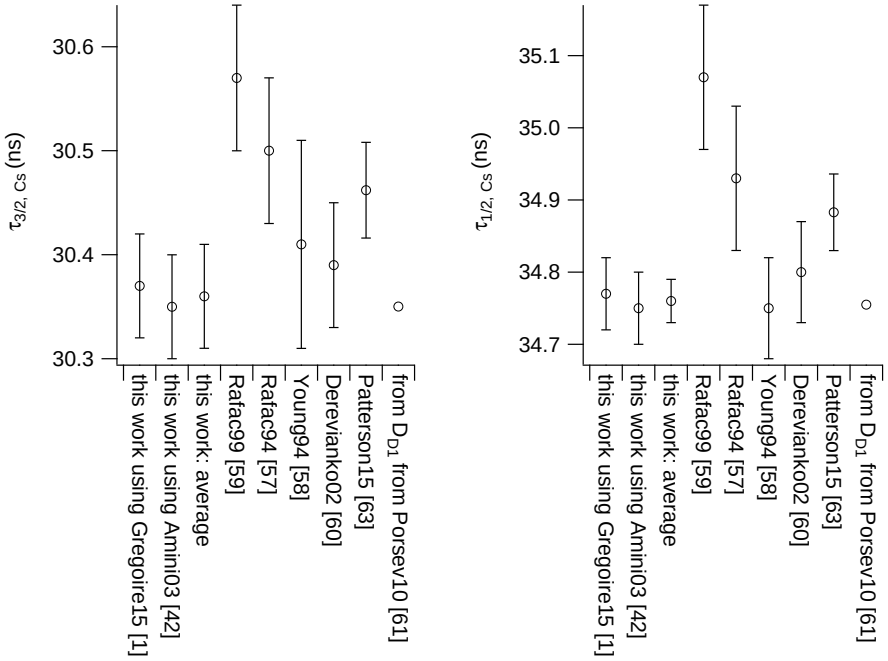

Figure 4. Comparisons of Cs principal transition lifetimes inferred from polarizability measurements [3,42] and theoretical $\alpha_{r,\mathrm{Cs}}(0)$ [47], direct measurements [57–60], and a combination of Porsev et *al.* 's calculated $|D_{D1}|$ [61] and R [52].

where r is the inter-nuclear distance and C_6, C_8, and C_{10} are dispersion coefficients that can be predicted based on $\alpha(0)$ measurements. For long-range interactions in the absence of retardation (i.e. for $a_0 \ll r \ll c/\omega_{D2}$), the C_6 term is most important. The C_6 coefficient for homo-nuclear atom-atom vdW interactions depends on dynamic polarizability as

$$C_6 = \frac{3\hbar}{\pi}\int_0^\infty [\alpha(i\omega)]^2\, d\omega \tag{19}$$

Even though $\hbar = 1$ in au, we write $\hbar$ explicitly in Eqn. (19) to emphasize that the dimensions of C_6 are energy $\times$ length^6.

The London result of $C_6 = (3/4)\hbar\omega_0\alpha(0)^2$ can be found from Eqn. (19) by using Eqn. (1) for $\alpha(i\omega)$ with a single term in the sum to represent an atom as a single oscillator of frequency ω_0 with static polarizability $\alpha(0)$. However, calculating C_6 gets more difficult for atoms with multiple oscillator strengths. In light of this complexity, we instead use the decomposition in Eqn. (5) to express C_6 as

$$\begin{aligned} C_6 &= \frac{3\hbar}{\pi}\int_0^\infty \left[\alpha_p(i\omega) + \alpha_r(i\omega)\right]^2 d\omega \\ &= \frac{3\hbar}{\pi}\int_0^\infty \left[\alpha_p(i\omega)\right]^2 d\omega + \frac{6\hbar}{\pi}\int_0^\infty \alpha_p(i\omega)\alpha_r(i\omega)d\omega + \frac{3\hbar}{\pi}\int_0^\infty \left[\alpha_r(i\omega)\right]^2 d\omega \end{aligned} \tag{20}$$

Because of the cross term, the integration over frequency, and the way $\alpha(i\omega)$ remains relatively constant until ultraviolet frequencies, α_r is significantly more important for C_6 than for $\alpha(0)$. Contributions from α_r account for 15% of C_6 whereas α_r contributes only 4% to $\alpha(0)$ for Cs, as pointed out by Derevianko et *al.* [33].

The fact that C_6 and $\alpha(0)$ depend on α_r in different ways [compare Eqns. (5) and (20)] suggests that it is possible to determine $\alpha_r(0)$ based on independent measurements of C_6 and $\alpha(0)$. We will explore this in Section 4. First, we want to demonstrate how to use experimental $\alpha(0)$ measurements

and theoretical $\alpha_r(i\omega)$ spectra to improve predictions of C_6 coefficients. For this we begin by factoring $\alpha_p(0)$ out of the $\alpha_p(i\omega)$ term in the integrand of Eqn. (20) to get

$$C_6 = \frac{3\hbar}{\pi}\int_0^\infty \left[\alpha_p(0)\frac{\alpha_p(i\omega)}{\alpha_p(0)} + \alpha_r(i\omega)\right]^2 d\omega \tag{21}$$

where the spectral shape function

$$\frac{\alpha_p(i\omega)}{\alpha_p(0)} = \frac{\frac{1}{\omega_{D1}^2+\omega^2} + \frac{R\frac{\omega_{D1}}{\omega_{D3}}}{\omega_{D3}^2+\omega^2}}{\frac{1}{\omega_{D1}^2} + \frac{R\frac{\omega_{D1}}{\omega_{D3}}}{\omega_{D3}^2}} \tag{22}$$

uses R defined in Eqn. (17). We are now able to calculate C_6 using our choice of $\alpha_p(0)$, which we can relate to static polarizability measurements via $\alpha_p(0) = \alpha(0) - \alpha_r(0)$. The formula for C_6 can then be written as

$$C_6 = \frac{3\hbar}{\pi}\int_0^\infty \left[[\alpha(0) - \alpha_r(0)]\frac{\alpha_p(i\omega)}{\alpha_p(0)} + \alpha_r(i\omega)\right]^2 d\omega \tag{23}$$

To use Eqn. (23) to infer values of C_6 from our static polarizability measurements, one still needs to know $\alpha_r(i\omega)$ and $\alpha_r(0)$. Derevianko et *al.* calculated and tabulated values $\alpha_{tab}(i\omega)$ in [64] of polarizability for all the alkali atoms, where the principal component $\alpha_p(i\omega)$ was calculated using experimental lifetime measurements by Volz and Schmoranzer [50] for Li, Na, K, and Rb and by Rafac et *al.* [57] for Cs. Therefore, we know that the residual component $\alpha_r(i\omega)$ of Derevianko et *al.*'s tabulated values of $\alpha_{tab}(i\omega)$ is

$$\alpha_r(i\omega) = \alpha_{tab}(i\omega) - 2\pi\epsilon_0 c^3\left[\frac{\tau_{1/2}^{-1}\omega_{D1}^{-2}}{\omega_{D1}^2-\omega^2} + 2\frac{\tau_{3/2}^{-1}\omega_{D2}^{-2}}{\omega_{D2}^2-\omega^2}\right] \tag{24}$$

Fig. 5 shows an example of how $\alpha_{tab}(i\omega)$ for Cs tabulated by Derevianko et *al.* [64] can be decomposed into principal and residual parts. Fig. 5 also shows the small adjustment to $\alpha_p(i\omega)$ that can be recommended based on measurements of $\alpha(0)$. In essence, this procedure makes the assumption that any deviation between the measured and the tabulated [64] values of static polarizability are due to an error in the α_p part of the tabulated values, and that the $\alpha_r(i\omega)$ component of the tabulated values is correct. To assess the impact of this assumption, next we examine how uncertainty in $\alpha_r(i\omega)$ propagates to uncertainty in C_6.

Equation (23) shows how C_6 calculations depend on $\alpha_r(0)$ and $\alpha(i\omega)$ with opposite signs. This helps explain why uncertainty in α_r propagates to uncertainty in C_6 with a somewhat reduced impact. For example, if α_r accounts for 15% of C_6, and α_r itself has an uncertainty of 5%, one might naievely expect that uncertainty in C_6 due to uncertainty in α_r would be 0.75%. However, using Eqn. (23) one can show that the uncertainty in C_6 is smaller (only 0.48% due to α_r). To explain this, if a theoretical α_r is incorrect, say a bit too high, then when we subtract this from the measured $\alpha(0)$ we will deduce an $\alpha_p(0)$ that is too small, and the error from this contribution to C_6 has the opposite sign from the error caused by adding back $\alpha_r(i\omega)$ in (23).

We can also rewrite Eqn. (23) by adding and subtracting the tabulated $\alpha_p(i\omega)$ so that C_6 depends explicitly only on the measured and tabulated (total) polarizabilities.

$$C_6 = \frac{3\hbar}{\pi}\int_0^\infty \left[[\alpha(0) - \alpha_{tab}(0)]\frac{\alpha_p(i\omega)}{\alpha_p(0)} + \alpha_{tab}(i\omega)\right]^2 d\omega \tag{25}$$

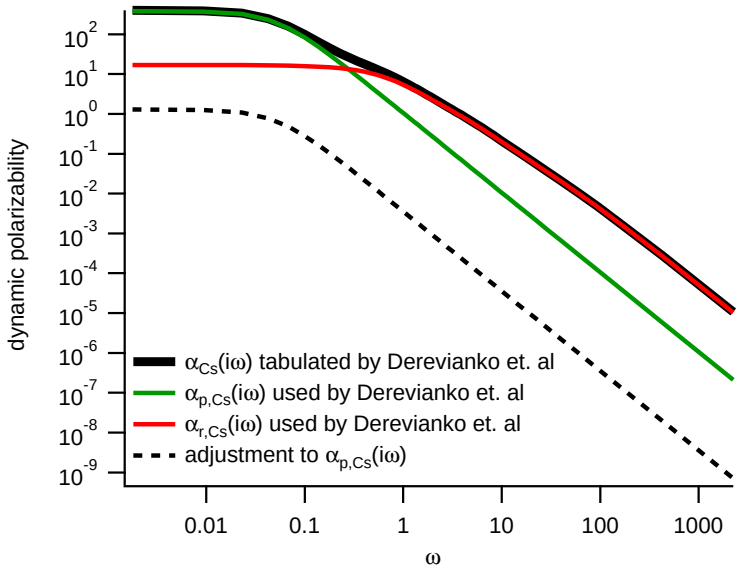

Figure 5. Cesium atom $\alpha_{tab}(i\omega)$ tabulated in [64] (black line), and its decomposition into calculated $\alpha_p(i\omega)$ based on $\tau_{1/2}$ and $\tau_{3/2}$ values [50] with Eq. (2) (green line) and the residual $\alpha_r(i\omega)$ (red line). The black dotted line represents the adjustment to $\alpha_p(i\omega)$ when we substitute $\alpha(0)$ measurement into Eqn. (23).

where $\alpha_{tab}(i\omega)$ and $\alpha_{tab}(0)$ refer to values tabulated by Derevianko et *al.* This way C_6 does not explicitly depend on α_r.

Using Eqn. (25), or equivalently Eqns. (23) and (24), our calculated C_6 values for Rb and Cs agree with recent theoretical and experimental C_6 values, as shown in Fig. 6. For K, our predicted C_6 is different from that measured by D'Errico et *al.* using Feshbach resonances by roughly 3σ. Of course, this discrepancy may be at least partly explained by statistical errors in the C_6 and $\alpha(0)$ measurements for K atoms. In the next section, however, we will explore how error in $\alpha_r(i\omega)$ used to construct $\alpha_{tab}(i\omega)$ for K could partly explain this discrepancy.

To interpret the C_6 values that we report in Table 4, we compare these semi-empirical results to direct measurements and earlier predictions of C_6 in Fig. 6. One sees that the uncertainty of C_6 measurements that we report based on atom interferometry measurements of polarizability are

Table 4. Homonuclear van der Waals C_6 coefficients, in atomic units, calculated using experimental static polarizabilities shown in Table 1 and tabulated dynamic polarizabilities from [64]. The two contributions to the uncertainty $\delta_{\alpha(0)}$ and $\delta_{\alpha_r(0)}$ for each C_6 value are, respectively, due to the uncertainties in measured $\alpha(0)$ and uncertainties estimated for Derevianko et *al.*'s values for $\alpha_r(i\omega)$ used to calculate $\alpha_{tab}(i\omega)$. Derevianko et *al.* [33] reported uncertainty in $\alpha_r(0)$ by using "an estimated 5% error for the core polarizabilities, and a 10% error for the remaining contributions to $\alpha_r(0)$." Several other authors also estimate 5% or 2% error for $\alpha_{\rm core}$.

Atom	C_6	$\delta_{\alpha(0)}$	$\delta_{\alpha_r(0)}$
Na	1558(11)	10	1
K	3884(16)	7	14
Rb	4724(31)	10	130
Cs	6879(15)	13	7

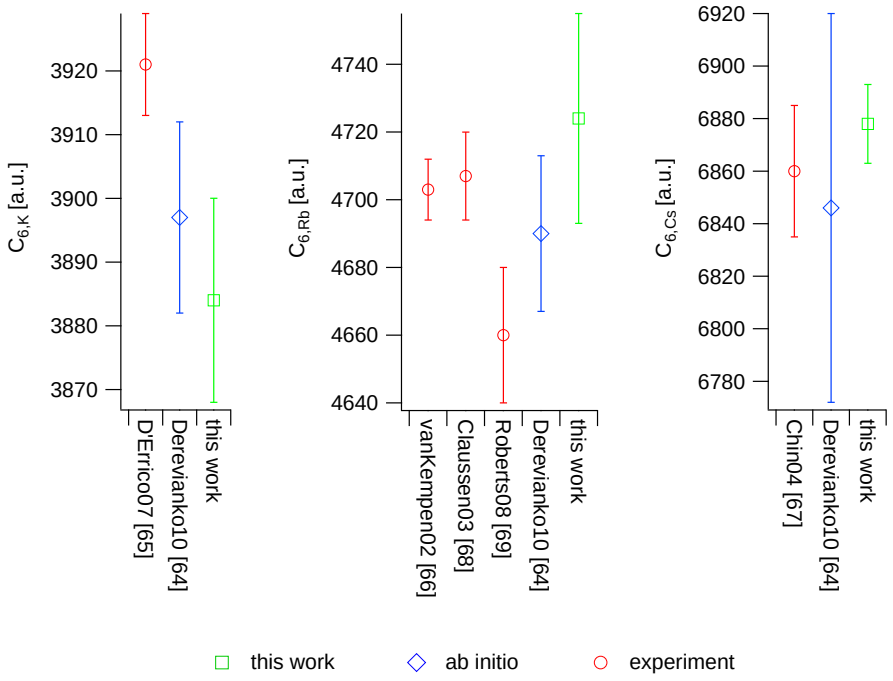

Figure 6. Theoretical [64] and experimental [65–69] C_6 values of K, Rb, and Cs from several different sources and the C_6 values determined in this article from polarizability measurements [3]. The experimental C_6 values were all determined from Feshbach resonance data.

comparable to direct measurements [65–67] and slightly more precise than previous semi-empirical predictions [64] .

4. Determining residual polarizabilities empirically

4.1. Using combinations of $\alpha(0)$ and τ measurements to report α_r values

While in Section 3 we demonstrated how to report atomic lifetimes from polarizability measurements and theoretical values for $\alpha_r(0)$, here we invert this procedure and use combinations of $\alpha(0)$, $\tau_{1/2}$, and $\tau_{3/2}$ measurements to place constraints on $\alpha_r(0)$. For this, we solve Eqn. (8) for $\alpha_r(0)$:

$$\alpha_r(0) = \alpha(0) - 2\pi\epsilon_0 c^3 \left[\frac{\tau_{1/2}^{-1}}{\omega_{D1}^4} + 2\frac{\tau_{3/2}^{-1}}{\omega_{D2}^4}\right] \tag{26}$$

Fig. 7 shows the difference between polarizability measurements $\alpha(0)$ and the inferred contribution to polarizability from the principal transitions $\alpha_p(0)$ based on lifetime measurements. We take the weighted average of $\alpha_p(0)$ based on a collection of available lifetime measurements, and we use the weighted average of the two high-precision $\alpha_{Cs}(0)$ measurements. We obtain $\alpha_{r,Li}(0)$ = 2(1), $\alpha_{r,Na}(0)$ = 2.0(5), $\alpha_{r,K}(0)$ = 5.4(4), $\alpha_{r,Rb}(0)$ = 11.4(5), and $\alpha_{r,Cs}(0)$ = 18.1(5). This analysis shows significantly nonzero $\alpha_r(0)$ values for Li, Na, K, Rb, and Cs based entirely on experimental data.

For Cs, this approach is sufficiently precise to empirically measure $\alpha_r(0)$ with 3% uncertainty, which is similar to the uncertainty of theoretical values [47,48]. The width of the blue and red bands in Fig. 7 indicate the contributions to this uncertainty from the atom interferometry polarizability

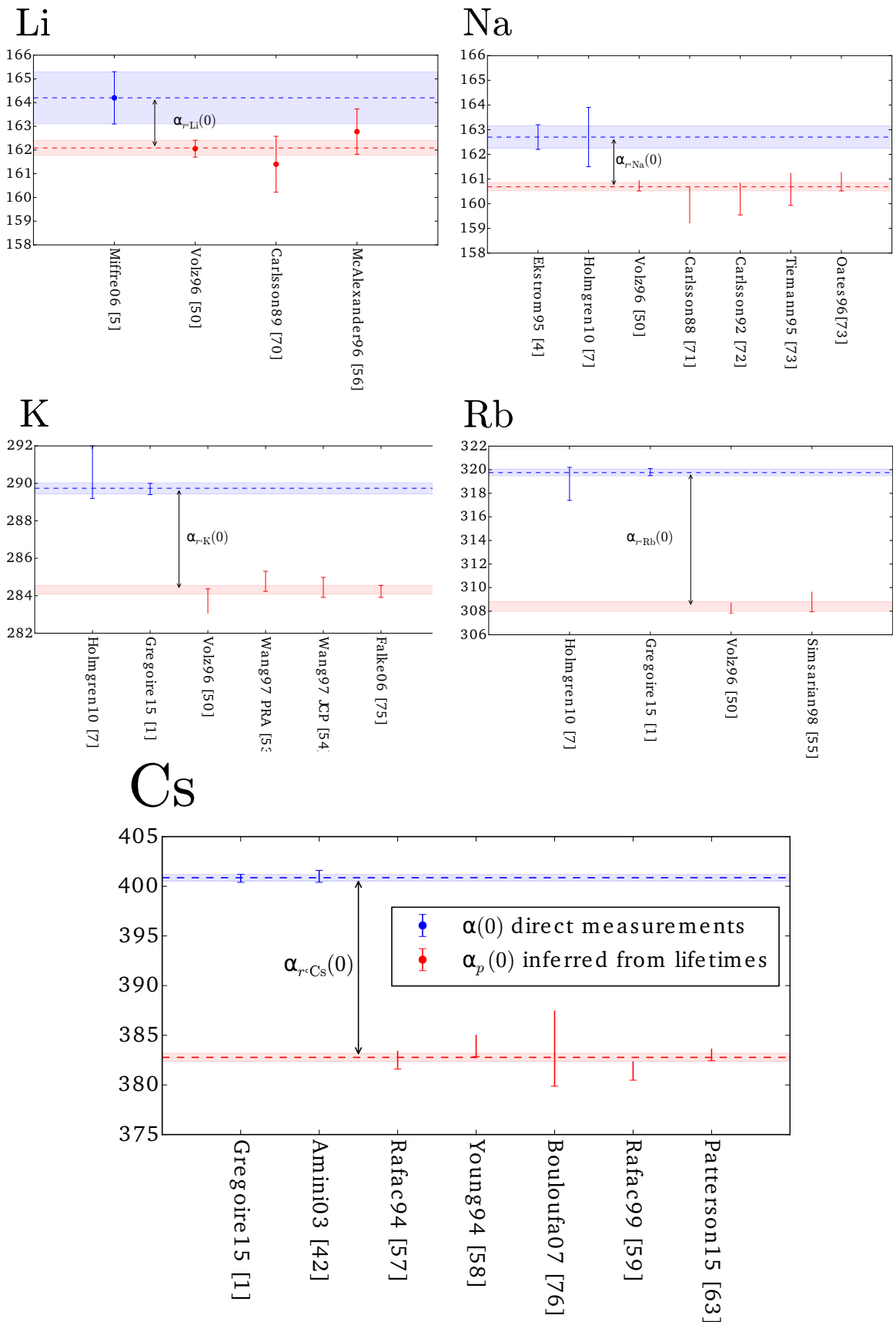

Figure 7. Differences between recent $\alpha(0)$ measurements [3–5,7,42] and an average of $\alpha_{p,\mathrm{Cs}}$ values calculated from lifetime measurements [50,53–59,63,70–76] and R values [12,18,50–52]. The uncertainties on those averages are used to calculate the resulting uncertainties in $\alpha_r(0)$.

measurements and the uncertainty contributions from lifetime measurements. In order to improve the accuracy of $\alpha(0)$ reported this way one would require improvements in both the polarizability measurements and the lifetime measurements.

We can use a similar approach by combining polarizability measurements with *ab initio* $|D_{ik}|$ calculations. One of the highest-accuracy calculations of $|D_{D1}|$ was reported for Cs by Porsev et *al.* [61] in order to help interpret atomic parity violation experiments. This $|D_{D1}|$ can be combined with R [52] using equations (9) and (17) as

$$\alpha_r(0) = \alpha(0) - \frac{|D_{D1}|^2}{3\hbar}\left[\frac{1}{\omega_{D1}} + \frac{R}{\omega_{D2}}\right] \tag{27}$$

This approach produces a somewhat lower value of $\alpha_r(0)$ = 16.5(4) with about 2.5% uncertainty. We compare the results using lifetimes and this result using the ratio of line strengths (R) and a calculated dipole matrix element with other results in Fig. 9 at the end of this section.

4.2. Using combinations of $\alpha(0)$ and C_6 measurements to report α_r values

Earlier in Section 3.2 we demonstrated how to calculate van der Waals C_6 coefficients from polarizability measurements and assumptions about residual polarizabilities. We can also invert this procedure, and analyze combinations of $\alpha(0)$ and C_6 measurements in order to place constraints on $\alpha_r(0)$. For this we will assume the spectral function $\alpha_r(i\omega)/\alpha_r(0)$ is sufficiently known and simply factor out an overall scale factor for the static residual polarizability from the formula for C_6 Eqn. (23) as follows:

$$C_6 = \frac{3\hbar}{\pi}\int_0^\infty \left[(\alpha(0) - \alpha_r(0))\frac{\alpha_p(i\omega)}{\alpha_p(0)} + \alpha_r(0)\frac{\tilde{\alpha}_r(i\omega)}{\tilde{\alpha}_r(0)}\right]^2 d\omega \tag{28}$$

where $\tilde{\alpha}_r(i\omega)$ and $\tilde{\alpha}_r(0)$ refer to values we infer from Eqn. (24) using values tabulated by Derevianko et *al.* We then plot predictions for C_6 versus predictions for $\alpha(0)$ parametric in hypothetical $\alpha_p(0)$ for different values of $\alpha_r(0)$. This is shown in Fig. 8 along with measurements of C_6 (red) and $\alpha(0)$ (blue). Even on the graph with a large domain (small plots in Fig. 8) where one sees the generally quadratic dependence of C_6 on $\alpha(0)$, it is evident that a model with $\alpha_r(0)$=0 is incompatible with the data. On the expanded region of interest (larger plots in Fig. 8), one sees the intersection of C_6 and $\alpha(0)$ measurements specifies a value of $\alpha_r(0)$. For Cs, we obtain an $\alpha_r(0)$ = 16.8(8) that is consistent with $\alpha_r(0)$ found from the other two methods we have presented so far in Section 4. This method is valuable because it relies on independent measurements of C_6 and $\alpha(0)$ to provide an empirical measurement of the size of α_r.

These plots show the values of $\alpha_r(0)$ and the corresponding uncertainties that we would infer using experimental values (and their uncertainties) of $\alpha(0)$ and C_6. From these studies we find a best fit $\alpha_r(0)$ of 8.0(4) for K, 9.6(4) for Rb, and 16.8(8) for Cs. The analysis for K highlights how the discrepancy between D'Errico et *al.*'s [65] $C_{6,\mathrm{K}}$ measurement and the $C_{6,\mathrm{K}}$ that we infer from our $\alpha(0)$ measurement [3] could be explained in part by error in assumed $\alpha_{\mathrm{K}}(0)$.

Fig. 9a shows the $\alpha_{r,\mathrm{Cs}}(0)$ values we inferred from lifetime measurements, van der Waals C_6 coefficients, and Porsev et *al.*'s calculated $|D_{D1,\mathrm{Cs}}|$. Our results are compared to *ab initio* calculations of $\alpha_{r,\mathrm{Cs}}(0)$ [47,48,64] as well as *ab initio* calculations of $\alpha_{\mathrm{core,Cs}}$ [77–81] to which we added $\alpha_{v'} + \alpha_{cv}$. Also among the comparisons in Fig. 9a are measurements of Cs^+ ionic polarizability [82–85], which approximates $\alpha_{\mathrm{core,Cs}}$, again adjusted by adding $\alpha_{v'} + \alpha_{cv}$. Fig. 9b shows our results alongside the *ab initio* $\alpha_r(0)$ values calculated by Safronova et *al.* [48] and Derevianko and Porsev [47] for Li, Na, K, Rb, and Cs.

Fig. 9 shows some disagreement between our $\alpha(0) + \tau$ and $\alpha(0) + C_6$ methods, especially with regard to K and Rb. There are several possible contributors to such disagreement. While the $\alpha(0) + \tau$ results were based on an average of several, independently-measured lifetimes, both of our methods

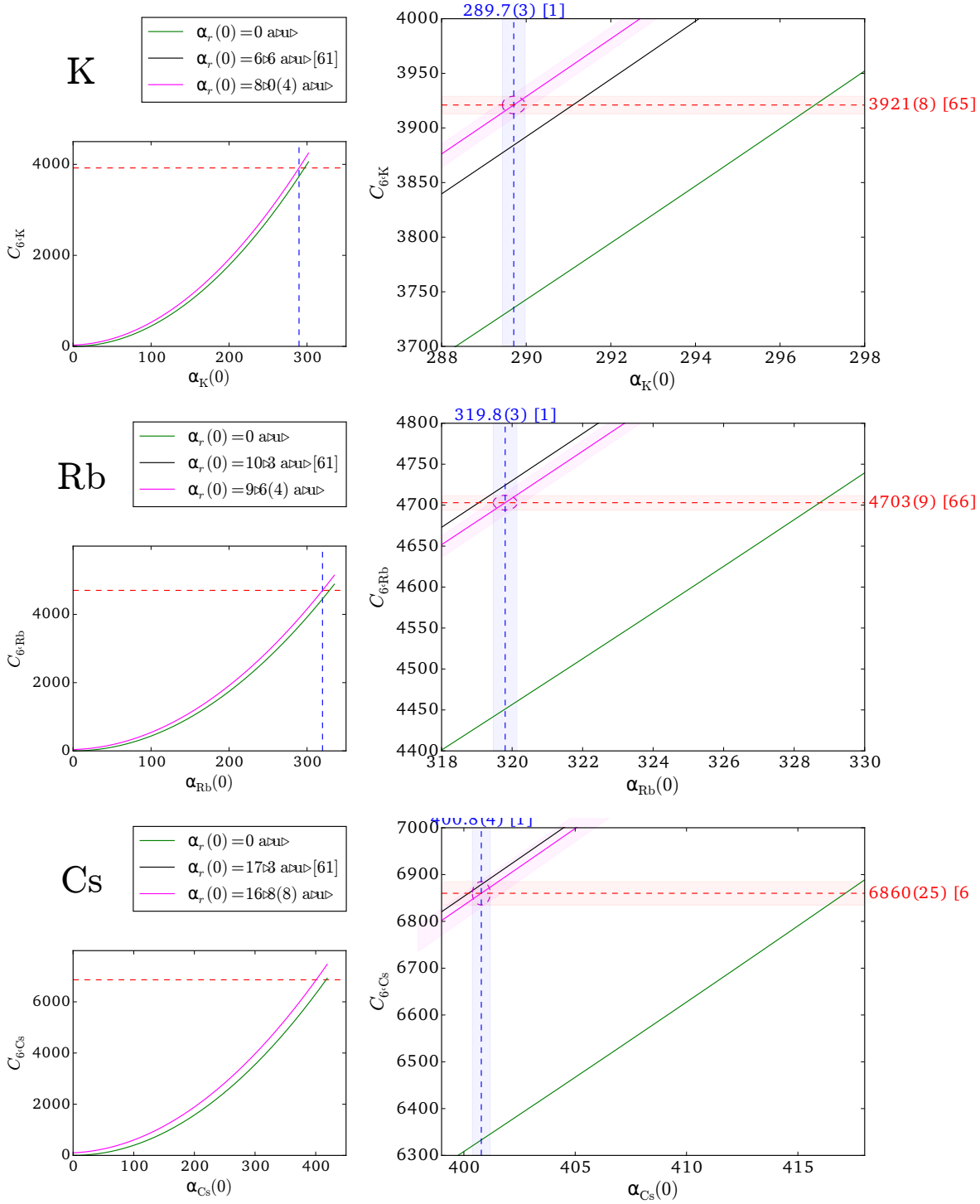

Figure 8. C_6 versus $\alpha(0)$ for small deviations about experimental values of $\alpha(0)$ [3]. The different curves correspond to different values of $\alpha_r(0)$: The pink curve corresponds to the value of $\alpha_r(0)$ inferred from experimental measurements of C_6 and $\alpha(0)$ [3], and the error bands on that curve represent the resulting uncertainty in $\alpha_r(0)$ due to uncertainty in C_6 and $\alpha(0)$. The black curve corresponds to the values of $\alpha(i\omega)$ tabulated by Derevianko et *al.* [64]. Finally, the green line corresponds to $\alpha_r(0) = 0$, and the inset on each plot shows C_6 versus $\alpha(0)$ for a wider range of $\alpha(0)$. For these plots, we used the $C_{6,K}$ measurement by D'Errico et *al.* [65], $C_{6,Rb}$ by van Kempen et *al.* [66], and $C_{6,Cs}$ by Chin et *al.* [67]. In the smaller plots, we can see that C_6 versus $\alpha(0)$ is approximately quadratic.

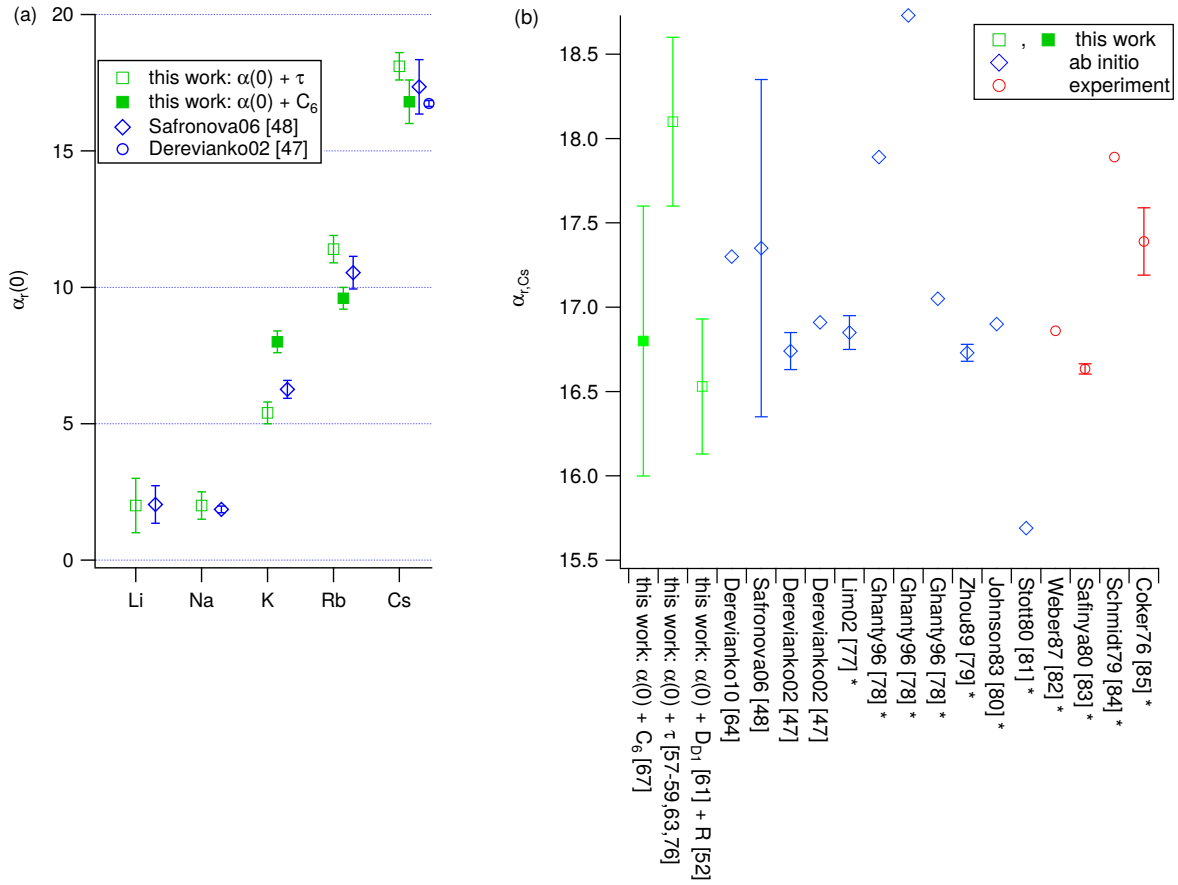

Figure 9. (a): $\alpha_r(0)$ values deduced by combining $\alpha(0)$ measurements [3–5,7,42] with either C_6 measurements [65–67] or principal transition lifetime measurements [50,53–59,63,70–76] and R values [12,18,50–52]. These inferred values are compared to the theoretical $\alpha_r(0)$ values we used elsewhere in this work by Safronova et *al.* [48] and Derevianko and Porsev [47]. (b): $\alpha_{r,\mathrm{Cs}}(0)$ values deduced by combining measured $\alpha_{\mathrm{Cs}}(0)$ [3] with either measured $C_{6,\mathrm{Cs}}$ [67], principal transition lifetime [57–59,63,76] and R_{Cs} [52] measurements, or $\alpha_{p,\mathrm{Cs}}(0)$ inferred from calculated $|D_{\mathrm{D1,Cs}}|$ [61] and measured R_{Cs} [52]. These inferred values are compared to several theoretical calculations [47,48,64,77–81] and Cs ion polarizability measurements [82–85]. The asterisk (*) indicates that the indicated references provided α_{core} values which we converted to $\alpha_r(0)$ values by adding $\alpha_{v'} + \alpha_{cv} = 1.81 - 0.72 = 1.09$ (in atomic units).

Table 5. $\alpha_r(0)$ values deduced by combining $\alpha(0)$ measurements [3–5,7,42] with either C_6 measurements [65–67], principal transition lifetime measurements [50,53–59,63,70–76] and R values [12,18,50–52], or $|D_{D1}|$ [61] and R values [52]. These inferred values are compared to the theoretical $\alpha_r(0)$ values we used elsewhere in this work by Safronova et *al.* [48] and Derevianko and Porsev [47].

atom	$\alpha(0)+\tau$ [$+R$]	$\alpha(0)+C_6$	$\alpha(0)+\lvert D_{D1}\rvert+R$	*ab initio*	
Li	2(1)			2.04(69) [48]	
Na	2.0(5)			1.86(12) [48]	
K	5.4(4)	8.0(4)		6.23(33) [48]	
Rb	11.4(5)	9.6(4)		10.54(60) [48]	
Cs	18.1(5)	16.8(8)	16.5(4)	17.35(100) [48]	16.74(11) [47]

relied on only one (or, in the case of Cs, two) $\alpha(0)$ measurements and our $\alpha(0) + C_6$ method relied on a single C_6 measurement. Therefore, statistical variation or systematic errors that were not accounted for in those $\alpha(0)$ or C_6 measurements could have a significant effect on our reported $\alpha_r(0)$. Also, it is important to note that our $\alpha(0) + C_6$ method relied on a single set of $\alpha(i\omega)$ calculated using one specific theoretical approach [64], and that there are other theoretical approaches that could lead to different values of $\alpha(i\omega)$.

The uncertainties in *ab initio* $\alpha_r(0)$ predictions by Safronova et *al.* [48] and Derevianko and Porsev [47] are comparable to or smaller than the uncertainties on our fully-empirical ($\alpha(0) + \tau$) and semi-empirical ($\alpha(0) + C_6$) results. This fact, combined with the aforementioned possible contributors to disagreement between our results, suggests that *ab initio* methods are still the prefered way of obtaining $\alpha_r(0)$ values for use in other analyses. Even so, it is valuable to develop the methods of analysis demonstrated in this paper so that when more accurate $\alpha(0)$, τ, and C_6 measurements become available, then $\alpha_r(0)$ can be determined with higher accuracy using these methods.

The theoretical $\alpha_r(0)$ predictions by Safronova et al. [48] have an uncertainty of 6%, which is just slightly larger than the 5% or 3% uncertainties of the experimental $\alpha_r(0)$ determinations that we reported for Cs in Sections 4.1 and 4.2. However, we acknowledge that there is a 10% deviation between the all-experimental result for $\alpha_{r,\mathrm{Cs}}(0)$ reported in Section 4.1 using $\alpha(0)$ and τ measurements as compared to the semi-empirical result for $\alpha_{r,\mathrm{Cs}}(0)$ that we reported in Section 4.2 using $\alpha(0)$ and C_6 measurements combined with the theoretical spectral function $\alpha_r(i\omega)/\alpha_r(0)$. Furthermore, the uncertainty in the theoretical $\alpha_{r,\mathrm{Cs}}(0)$ prediction by Derevianko and Porsev [47] is significantly smaller, approximately 0.6% (and this was partly verified with independent measurements of α_{core} using Rydberg spectroscopy [79]). So, it is possible that ab initio methods are still the preferred way of obtaining $\alpha_r(0)$ values for use in other analyses. Even so, we conclude that it is valuable to develop the methods of analysis demonstrated in this paper so that when more accurate $\alpha(0)$, τ, and C_6 measurements become available, then $\alpha_r(0)$ can be determined with higher accuracy using these methods. In the future, combining measurements of α_{core} from Rydberg spectroscopy with higher accuracy measurements of $\alpha_r(0)$ could provide more direct constraints on $\alpha_{v'} + \alpha_{cv}$, and thus α_{tail}.

5. Discussion

In this paper we reported measurements of the static polarizabilities of K, Rb, and Cs atoms with reduced uncertainties. We made these measurements with an atom interferometer and an electric field gradient using data originally reported in [1]. We described in Section 2 how we reduced the systematic uncertainty in $\alpha(0)$ measurements from 0.15% to 0.10% by improving the calibration of the electric field. To our knowledge, these are now the most precise measurements of atomic polarizabilities that have been made using any method for K, Rb, and Cs atoms. For Cs in particular, the improvement described in this paper enabled us to report a value of $\alpha_{\mathrm{Cs}}(0)$ with slightly smaller uncertainty than Amini and Gould's measurement of $\alpha_{\mathrm{Cs}}(0)$ that they obtained using an atomic fountain experiment [42]. Currently, this means that atom interferometer experiments have made the most accurate measurements of atomic polarizabilities for all of the alkali metal atoms Li, Na, K, Rb, and Cs.

In Section 3 we demonstrated how to analyze these measurements of atomic polarizabilities in order to infer oscillator strengths, lifetimes, transition matrix elements, line strengths, and van der Waals C_6 coefficients for all the alkali metal atoms, as we did in Tables 2 and 4. We referred to the idea chart in Fig. 1 to review how these quantities are interrelated, and we described this more explicitly with Eqns. 1-17 and 19-25. Building on these interrelationships, we specifically used measurements of static polarizabilities obtained with atom interferometry, empirical ratios of line strengths R (some of which were also obtained with atom interferometry), and theoretical values for residual polarizabilities in order to deduce the lifetimes of excited np_J states for all of the alkali metal atoms with unprecedented accuracy. These methods also allow us to use static polarizability

measurements as a semi-empirical benchmark to test *ab initio* predictions of principal ns-np_J transition matrix elements for alkali metal atoms. Furthermore, we used these methods to test the extent to which measurements of different atomic properties such as lifetimes, branching ratios, line strengths, polarizabilities, and van der Waals interactions agree with one another, as shown in Figs. 4 and 6.

Then in Section 4 we explored new methods to infer residual polarizability $\alpha_r(0)$ values by combining measurements of atomic polarizabilities with independent measurements of lifetimes or C_6 coefficients. This constitutes a novel, all-experimental method to test several theoretical $\alpha_r(0)$ predictions. Using this approach it is clear that atom interferometry measurements of atomic polarizabilities are sufficiently precise to detect non-zero residual polarizabilities for all of the alkali metal atoms, and can measure $\alpha_r(0)$ with as little as 3% uncertainty for Cs atoms. This procedure also provides a motivation for next generation C_6, $\alpha(0)$, τ, and tune-out wavelength measurements that can be combined with one another to more accurately determine $\alpha_r(0)$ values that are needed in order to test atomic structure calculations that are relevant for interpreting atomic parity violation and atomic clocks.

6. Acknowledgements

This work is supported by NSF Grant No. 1306308 and a NIST PMG. M.D.G. and R.T. are grateful for NSF GRFP Grant No. DGE-1143953 for support. N.B. acknowledges support from the NASA Space Grant Consortium at the University of Arizona.

Appendix A.

Table 6. Contributions to residual polarizability $\alpha_r(0) = \alpha_{v'}(0) + \alpha_{\rm core}(0) + \alpha_{cv}(0)$ in atomic units. The quantity $\alpha_{v'}(0)$ is the sum of all the contributions from the valence electron ns-$n'p_J$ transitions with $n' > n$ using Eqn. (1). This includes $\alpha_{\rm tail}(0)$. Values in bold are used to produce the results presented in Table 2 are in bold.

atom	$\alpha_{v'}(0)$	$\alpha_{\rm core}(0)$		$\alpha_{cv}(0)$	$\alpha_r(0)$	
Li		0.189(9)	[80] [b]		**2.04(69)**	[48]
Li		0.192	[86]			
Na	0.81 [a]	0.94(5)	[80] [b]			
Na		1.00(4)	[77]		**1.86(12)**	[48]
K	0.72 [a]	5.46(27)	[80] [b]			
K	0.90 [40]	5.50	[40]			
K		5.52(4)	[77]			
K		5.50	[87]	-0.18 [87]	**6.26(33)**	[48]
Rb	1.32 [a]	9.08(45)	[80] [b]			
Rb		9.11(4)	[77]		10.70(22)	[12] [c]
Rb		9.11(4)	[88]	-0.30 [88]	**10.54(60)**	[48]
Cs	1.60 [a]	15.8(8)	[80] [b]	-0.72 [47]	17.35(100)	[48]
Cs		15.8(1)	[77]		16.91	[47]
Cs	1.81 [47]	15.81	[47]		**16.74(11)**	[47]
Cs		16.3(2)	[85] [d]			
Cs		15.17	[89] [d]			
Cs		15.54(3)	[83] [e]			
Cs		15.82(3)	[90] [e]			
Cs		15.770(3)	[82] [e]			
Cs		17.64	[78] [f]			

[a] Calculated using f_{ik} values from NIST [49] for $n - n'$ transitions with $n' = n + 1$ to $n + 5$.
[b] For $\alpha_{\rm core}$ from [80] we list a fractional uncertainty of 5% as suggested in reference [88].
[c] Reference [12] calculated $(\alpha_{\rm core} + \alpha_{cv})$ = 8.71(9) and $\alpha_r = 10.70(22)$ at $\omega = 2\pi c/790$nm.
[d] from studies of ions in solid crystals
[e] from Rydberg spectroscopy data
[f] A result from DFT calculations

Bibliography

1. Berman, P., Ed. *Atom Interferometry*; Academic Press: San Diego, 1997.
2. Cronin, A.D.; Schmiedmayer, J.; Pritchard, D.E. Optics and interferometry with atoms and molecules. *Rev. Mod. Phys.* **2009**, *81*, 1051.
3. Gregoire, M.D.; Hromada, I.; Holmgren, W.F.; Trubko, R.; Cronin, A.D. Measurements of the ground-state polarizabilities of Cs, Rb, and K using atom interferometry. *Phys. Rev. A* **2015**, *92*, 052513.
4. Ekstrom, C.R.; Schmiedmayer, J.; Chapman, M.S.; Hammond, T.D.; Pritchard, D.E. Measurement of the electric polarizability of sodium with an atom interferometer. *Phys. Rev. A* **1995**, *51*, 3883.
5. Miffre, A.; Jacquey, M.; Büchner, M.; Trénec, G.; Vigué, J. Atom interferometry measurement of the electric polarizability of lithium. *Eur. Phys. J. D* **2006**, *38*, 353.
6. Berninger, M.; Stefanov, A.; Deachapunya, S.; Arndt, M. Polarizability measurements of a molecule via a near-field matter-wave interferometer. *Phys. Rev. A* **2007**, *76*, 013607.
7. Holmgren, W.F.; Revelle, M.C.; Lonij, V.P.A.; Cronin, A.D. Absolute and ratio measurements of the polarizability of Na, K, and Rb with an atom interferometer. *Phys. Rev. A* **2010**, *81*, 053607.
8. Perreault, J.D.; Cronin, A.D. Observation of atom wave phase shifts induced by van der Waals atom-surface interactions. *Phys. Rev. Lett.* **2005**, *95*, 133201.
9. Lepoutre, S.; Jelassi, H.; Lonij, V.P.A.; Trénec, G.; Büchner, M.; Cronin, a.D.; Vigué, J. Dispersive atom interferometry phase shifts due to atom-surface interactions. *Europhys. Lett.* **2009**, *88*, 20002.
10. Lepoutre, S.; Lonij, V.P.A.; Jelassi, H.; Trenec, G.; Buchner, M.; Cronin, A.D.; Vigue, J.; Trénec, G.; Büchner, M.; Vigué, J. Atom interferometry measurement of the atom-surface van der Waals interaction. *Eur. Phys. J. D* **2011**, *62*, 309.
11. Holmgren, W.F.; Trubko, R.; Hromada, I.; Cronin, A.D. Measurement of a wavelength of light for which the energy shift for an atom vanishes. *Phys. Rev. Lett.* **2012**, *109*, 243004.
12. Leonard, R.H.; Fallon, A.J.; Sackett, C.A.; Safronova, M.S. High-precision measurements of the ^{87}RbD-line tune-out wavelength. *Phys. Rev. A* **2015**, *92*, 052501.
13. Mitroy, J.; Safronova, M.S.; Clark, C.W. Theory and applications of atomic and ionic polarizabilities. *J. Phys. B* **2010**, *44*, 202001.
14. Tang, L.Y.; Yan, Z.C.; Shi, T.Y.; Babb, J.F. Nonrelativistic ab initio calculations for 2 S 2, 2 P 2, and 3 D 2 lithium isotopes: Applications to polarizabilities and dispersion interactions. *Physical Review A* **2009**, *79*, 062712.
15. Sahoo, B. An ab initio relativistic coupled-cluster theory of dipole and quadrupole polarizabilities: Applications to a few alkali atoms and alkaline earth ions. *Chemical Physics Letters* **2007**, *448*, 144–149.
16. Hamonou, L.; Hibbert, A. Static and dynamic polarizabilities of Na-like ions. *Journal of Physics B: Atomic, Molecular and Optical Physics* **2007**, *40*, 3555.
17. Deiglmayr, J.; Aymar, M.; Wester, R.; Weidemüller, M.; Dulieu, O. Calculations of static dipole polarizabilities of alkali dimers: Prospects for alignment of ultracold molecules. *The Journal of chemical physics* **2008**, *129*, 064309.
18. Johnson, W.; Safronova, U.; Derevianko, A.; Safronova, M. Relativistic many-body calculation of energies, lifetimes, hyperfine constants, and polarizabilities in Li 7. *Physical Review A* **2008**, *77*, 022510.
19. Reinsch, E.A.; Meyer, W. Finite perturbation calculation for the static dipole polarizabilities of the atoms Na through Ca. *Phys. Rev. A* **1976**, *14*, 915.
20. Tang, K.T. Upper and lower bounds of two- and three-body dipole, quadrupole, and octupole van der Waals coefficients for hydrogen, noble gas, and alkali atom interactions. *J. Chem. Phys.* **1976**, *64*, 3063.
21. Maeder, F.; Kutzelnigg, W. Natural states of interacting systems and their use for the calculation of intermolecular forces (IV) Calculation of van der Waals coefficients between one-and two-valence-electron atoms in their ground states, as well as of polarizabilities, oscillator strength sums and related quantities, including correlation effects. *Chemical Physics* **1979**, *42*, 95–112.
22. Christiansen, P.A.; Pitzer, K.S. Reliable static electric dipole polarizabilities for heavy elements. *Chem. Phys. Lett.* **1982**, *85*, 434.
23. Fuentealba, P. On the reliability of semiempirical pseudopotentials: dipole polarisability of the alkali atoms. *Journal of Physics B: Atomic and Molecular Physics* **1982**, *15*, L555.

24. Müller, W.; Flesch, J.; Meyer, W. Treatment of intershell correlation effects in *ab initio* calculations by use of core polarization potentials. Method and application to alkali and alkaline earth atoms. *J. Chem. Phys.* **1984**, *80*, 3297.
25. Kundu, B.; Ray, D.; Mukherjee, P. Dynamic polarizabilities and Rydberg states of the sodium isoelectronic sequence. *Physical Review A* **1986**, *34*, 62.
26. Kello, V.; Sadlej, A.J.; Faegri, K. Electron-correlation and relativistic contributions to atomic dipole polarizabilities: Alkali-metal atoms. *Phys. Rev. A* **1993**, *47*, 1715.
27. Fuentealba, P.; Reyes, O. Atomic softness and the electric dipole polarizability. *J. Mol. Struct. THEOCHEM* **1993**, *282*, 65.
28. Marinescu, M.; Sadeghpour, H.; Dalgarno, A. Dispersion coefficients for alkali-metal dimers. *Physical Review A* **1994**, *49*, 982.
29. Dolg, M. Fully relativistic pseudopotentials for alkaline atoms: Dirac–Hartree–Fock and configuration interaction calculations of alkaline monohydrides. *Theor. Chim. Acta* **1996**, *93*, 141.
30. Patil, S.H.; Tang, K.T. Multipolar polarizabilities and two- and three-body dispersion coefficients for alkali isoelectronic sequences. *J. Chem. Phys.* **1997**, *106*, 2298.
31. Lim, I.S.; Pernpointner, M.; Seth, M.; Laerdahl, J.K.; Schwerdtfeger, P.; Neogrady, P.; Urban, M. Relativistic coupled-cluster static dipole polarizabilities of the alkali metals from Li to element 119. *Phys. Rev. A* **1999**, *60*, 2822.
32. Safronova, M.S.; Johnson, W.R.; Derevianko, A. Relativistic many-body calculations of energy levels, hyperfine constants, electric-dipole matrix elements and static polarizabilities for alkali-metal atoms. *Phys. Rev. A* **1999**, *60*, 27.
33. Derevianko, A.; Johnson, W.R.; Safronova, M.S.; Babb, J.F. High-precision calculations of dispersion coefficients, static dipole polarizabilities, and atom-wall interaction constants for alkali-metal atoms. *Phys. Rev. Lett.* **1999**, *82*, 3589.
34. Magnier, S.; Aubert-Frécon, M. Static dipolar polarizabilities for various electronic states of alkali atoms. *J. Quant. Spectrosc. Radiat. Transf.* **2002**, *75*, 121.
35. Mitroy, J.; Bromley, M.W.J. Semiempirical calculation of van der Waals coefficients for alkali-metal and alkaline-earth-metal atoms. *Phys. Rev. A* **2003**, *68*, 052714.
36. Safronova, M.S.; Clark, C.W. Inconsistencies between lifetime and polarizability measurements in Cs. *Phys. Rev. A* **2004**, *69*, 040501.
37. Lim, I.S.; Schwerdtfeger, P.; Metz, B.; Stoll, H. All-electron and relativistic pseudopotential studies for the group 1 element polarizabilities from K to element 119. *J. Chem. Phys.* **2005**, *122*, 104103.
38. Arora, B.; Safronova, M.; Clark, C.W. Determination of electric-dipole matrix elements in K and Rb from Stark shift measurements. *Physical Review A* **2007**, *76*, 052516.
39. Iskrenova-Tchoukova, E.; Safronova, M.S.; Safronova, U.I. High-precision study of Cs polarizabilities. *J. Comput. Methods Sci. Eng.* **2007**, *7*, 521.
40. Safronova, U.I.; Safronova, M.S. High-accuracy calculation of energies , lifetimes , hyperfine constants , multipole polarizabilities , and blackbody radiation shift in ^{39}K. *Phys. Rev. A* **2008**, *78*, 052504.
41. Safronova, M.S.; Safronova, U.I. Critically evaluated theoretical energies, lifetimes, hyperfine constants, and multipole polarizabilities in ^{87}Rb. *Phys. Rev. A* **2011**, *83*, 052508.
42. Amini, J.M.; Gould, H. High precision measurement of the static dipole polarizability of cesium. *Phys. Rev. Lett.* **2003**, *91*, 153001.
43. Schwerdtfeger, P. Atomic static dipole polarizabilities. In *Atoms, Mol. Clust. Electr. Fields Theor. Approaches to Calc. Electr. Polariz.*; 2006; pp. 1–32.
44. Schwerdtfeger, P. Table of experimental and calculated static dipole polarizabilities for the electronic ground states of the neutral elements (in atomic units). *Cent. Theor. Chem. Phys. (CTCP), New Zeal. Inst. Adv. Study, Massey Univ. Auckl.*
45. Gould, H.; Miller, T.M. *Recent Developments in the Measurement of Static Electric Dipole Polarizabilities*; Vol. 51, Elsevier Masson SAS, 2005; p. 343.
46. Haynes, W.M. *CRC Handbook of Chemistry and Physics*; CRC Press, 2014.
47. Derevianko, A.; Porsev, S.G. High-precision determination of transition amplitudes of principal transitions in Cs from van der Waals coefficient C_6. *Phys. Rev. A* **2002**, *65*, 053403.

48. Safronova, M.S.; Arora, B.; Clark, C.W. Frequency-dependent polarizabilities of alkali-metal atoms from ultraviolet through infrared spectral regions. *Phys. Rev. A* **2006**, *73*, 022505.
49. NIST. NIST Atomic Spectra Database.
50. Volz, U.; Schmoranzer, H. Precision lifetime measurements on alkali atoms and on helium by beam–gas–laser spectroscopy. *Phys. Scr.* **1996**, *T65*, 48.
51. Trubko, R. Precision tune-out wavelength measurements with an atom interferometer. *Prep.* **2016**.
52. Rafac, R.J.; Tanner, C.E. Measurement of the ratio of the cesium D-line transition strengths. *Phys. Rev. A* **1998**, *58*, 1087.
53. Wang, H.; Li, J.; Wang, X.T.; Williams, C.J.; Gould, P.L.; Stwalley, W.C. Precise determination of the dipole matrix element and radiative lifetime of the ^{39}K 4p state by photoassociative spectroscopy. *Phys. Rev. A* **1997**, *55*, R1569.
54. Wang, H.; Gould, P.L.; Stwalley, W.C. Long-range interaction of the ^{3}9K(4s)+^{3}9K(4p) asymptote by photoassociative spectroscopy. I. The 0^i_g pure long-range state and the long-range potential constants. *J. Chem. Phys.* **1997**, *106*, 7899.
55. Simsarian, J.E.; Orozco, L.A.; Sprouse, G.D.; Zhao, W.Z. Lifetime measurements of the $7p$ levels of atomic francium. *Phys. Rev. A* **1998**, *57*, 2448.
56. McAlexander, W.I.; Abraham, E.R.I.; Hulet, R.G. Radiative lifetime of the $2P$ state of lithium. *Phys. Rev. A* **1996**, *54*, R5.
57. Rafac, R.J.; Tanner, C.E.; Livingston, A.E.; Kukla, K.W.; Berry, H.G.; Kurtz, C.A. Precision lifetime measurements of the $6p^2P_{1/2,3/2}$ states in atomic cesium **1994**. *50*, 1976.
58. Young, L.; Hill, W.T.; Sibener, S.J.; Price, S.D.; Tanner, C.E.; Wieman, C.E.; Leone, S.R. Precision lifetime measurements of Cs $6p\,^2P_{1/2}$ and $6p\,^2P_{3/2}$ levels by single-photon counting. *Phys. Rev. A* **1994**, *50*, 2174.
59. Rafac, R.J.; Tanner, C.E.; Livingston, A.E.; Berry, H.G. Fast-beam laser lifetime measurements of the cesium 6p $^2P_{1/2,3/2}$ states. *Phys. Rev. A* **1999**, *60*, 3648.
60. Derevianko, A.; Porsev, S.G. Determination of lifetimes of 6 P J levels and ground-state polarizability of Cs from the van der Waals coefficient C 6. *Physical Review A* **2002**, *65*, 053403.
61. Porsev, S.G.; Beloy, K.; Derevianko, A. Precision determination of weak charge of ^{133}Cs from atomic parity violation. *Phys. Rev. D* **2010**, *82*, 036008.
62. Porsev, S.G.; Beloy, K.; Derevianko, A. Precision determination of electroweak coupling from atomic parity violation and implications for particle physics. *Phys. Rev. Lett.* **2009**, *102*, 181601.
63. Patterson, B.M.; Sell, J.F.; Ehrenreich, T.; Gearba, M.A.; Brooke, G.M.; Scoville, J.; Knize, R.J. Lifetime measurement of the cesium 6 P 3/2 level using ultrafast pump-probe laser pulses. *Physical Review A* **2015**, *91*, 012506.
64. Derevianko, A.; Porsev, S.G.; Babb, J.F. Electric dipole polarizabilities at imaginary frequencies for hydrogen, the alkali-metal, alkaline-earth, and noble gas atoms. *At. Data Nucl. Data Tables* **2010**, *96*, 323.
65. D'Errico, C.; Zaccanti, M.; Fattori, M.; Roati, G.; Inguscio, M.; Modugno, G.; Simoni, A. Feshbach resonances in ultracold K(39). *New J. Phys.* **2007**, *9*, 223.
66. van Kempen, E.G.M.; Kokkelmans, S.J.J.M.F.; Heinzen, D.J.; Verhaar, B.J. Interisotope determination of ultracold rubidium interactions from three high-precision experiments. *Phys. Rev. Lett.* **2002**, *88*, 093201.
67. Chin, C.; Vuletić, V.; Kerman, A.J.; Chu, S.; Tiesinga, E.; Leo, P.J.; Williams, C.J. Precision feshbach spectroscopy of ultracold Cs_2. *Phys. Rev. A* **2004**, *70*, 032701.
68. Claussen, N.R.; Kokkelmans, S.J.J.M.F.; Thompson, S.T.; Donley, E.A.; Hodby, E.; Wieman, C.E. Very-high-precision bound-state spectroscopy near a 85Rb Feshbach resonance. *Phys. Rev. A* **2003**, *67*, 060701.
69. Roberts, J.L.; Claussen, N.R.; Burke, J.P.; Greene, C.H.; Cornell, E.A.; Wieman, C.E. Resonant Magnetic Field Control of Elastic Scattering in Cold 85Rb. *Phys. Rev. Lett.* **1998**, *81*, 5109.
70. Carlsson, J.; Sturesson, L. Accurate time-resolved laser spectroscopy on lithium atoms. *Zeitschrift für Physik D Atoms, Molecules and Clusters* **1989**, *14*, 281–287.
71. Carlsson, J. Accurate time-resolved laser spectroscopy on sodium and bismuth atoms. *Zeitschrift für Physik D Atoms, Molecules and Clusters* **1988**, *9*, 147–151.
72. Carlsson, J.; Jönsson, P.; Sturesson, L.; Fischer, C.F. Multi-configuration Hartree-Fock calculations and time-resolved laser spectroscopy studies of hyperfine structure constants in sodium. *Physica Scripta* **1992**, *46*, 394.

73. Tiemann, E.; Knöckel, H.; Richling, H. Long-range interaction at the asymptote 3s+3 of Na2. *Zeitschrift für Physik D Atoms, Molecules and Clusters* **1996**, *37*, 323–332.
74. Oates, C.W.; Vogel, K.R.; Hall, J.L. High Precision Linewidth Measurement of Laser-Cooled Atoms: Resolution of the Na $3p^2P_{3/2}$ Lifetime Discrepancy. *Phys. Rev. Lett.* **1996**, *76*, 2866–2869.
75. Falke, S.; Sherstov, I.; Tiemann, E.; Lisdat, C. The $A^1\Sigma_u^+$ state of K_2 up to the dissociation limit. *J. Chem. Phys.* **2006**, *125*, 224303.
76. Bouloufa, N.; Crubellier, A.; Dulieu, O. Reexamination of the 0_g^- pure long-range state of Cs_2: Prediction of missing levels in the photoassociation spectrum. *Phys. Rev. A* **2007**, *75*, 052501.
77. Lim, I.S.; Laerdahl, J.K.; Schwerdtfeger, P. Fully relativistic coupled-cluster static dipole polarizabilities of the positively charged alkali ions from Li+ to 119+. *J. Chem. Phys.* **2002**, *116*, 172.
78. Ghanty, T.K.; Ghosh, S.K. A new simple approach to the polarizability of atoms and ions using frontier orbitals from the Kohn-Sham density functional theory. *Journal of Molecular Structure: THEOCHEM* **1996**, *366*, 139–144.
79. Zhou, H.L.; Norcross, D.W. Improved calculation of the quadratic Stark effect in the $6P_{3/2}$ state of Cs. *Phys. Rev. A* **1989**, *40*, 5048–5051.
80. Johnson, W.; Kolb, D.; Huang, K.N. Electric-dipole, quadrupole, and magnetic-dipole susceptibilities and shielding factors for closed-shell ions of the He, Ne, Ar, Ni (Cu^+), Kr, Pb, and Xe isoelectronic sequences. *At. Data Nucl. Data Tables* **1983**, *28*, 333.
81. Stott, M.J.; Zaremba, E. Linear-response theory within the density-functional formalism: Application to atomic polarizabilities. *Phys. Rev. A* **1980**, *21*, 12–23.
82. Weber, K.H.; Sansonetti, C.J. Accurate energies of nS , nP , nD , nF , and nG levels of neutral cesium. *Phys. Rev. A* **1987**, *35*, 4650–4660.
83. Safinya, K.; Gallagher, T.; Sandner, W. Resonance measurements of f- h and f- i intervals in cesium using selective and delayed field ionization. *Physical Review A* **1980**, *22*, 2672.
84. Schmidt, P.C.; Weiss, A.; Das, T.P. Effect of crystal fields and self-consistency on dipole and quadrupole polarizabilities of closed-shell ions. *Phys. Rev. B* **1979**, *19*, 5525–5534.
85. Coker, H. Empirical Free-Ion Polarizabilities of the Alkali Metal, Alkaline Earth Metal, and Halide Ions. *J. Phys. Chem.* **1976**, *80*, 2078.
86. Johnson, W.; Cheng, K. Relativistic configuration-interaction calculation of the polarizabilities of heliumlike ions. *Physical Review A* **1996**, *53*, 1375.
87. Safronova, M.S.; Safronova, U.I.; Clark, C.W. Magic wavelengths for optical cooling and trapping of potassium. *Phys. Rev. A* **2013**, *87*, 052504.
88. Safronova, M.S.; Williams, C.J.; Clark, C.W. Relativistic many-body calculations of electric-dipole matrix elements, lifetimes and polarizabilities in rubidium **2004**. *69*, 022509.
89. Rosseinsky, D.R. An electrostatics framework relating ionization potential (and electron affinity), electronegativity, polarizability, and ionic radius in monatomic species. *Journal of the American Chemical Society* **1994**, *116*, 1063–1066.
90. Ruff, G.; Safinya, K.; Gallagher, T. Measurements of the n= 15- 17 f- g intervals in Cs. *Physical Review A* **1980**, *22*, 183.

© 2016 by the authors. Submitted to *Atoms* for possible open access publication under the terms and conditions of the Creative Commons Attribution license (http://creativecommons.org/licenses/by/4.0/)